AD NUMBER
AD224446
CLASSIFICATION CHANGES
TO: unclassified
FROM: confidential
LIMITATION CHANGES
TO: Approved for public release, distribution unlimited
FROM: Distribution authorized to U.S. Gov't. agencies and their contractors; Administrative/Operational Use; 04 SEP 1958. Other requests shall be referred to National Aeronautics and Space Administration, Washington, DC.
AUTHORITY
17 Jul 1962, NASA TR Server Website; 17 Jul 1962, NASA TR Server Website

[redacted] Copy 23
RM E58E20

RESEARCH MEMORANDUM

COMPARISON OF CALCULATED AND EXPERIMENTAL TEMPERATURES AND COOLANT PRESSURE LOSSES FOR A CASCADE OF SMALL AIR-COOLED TURBINE ROTOR BLADES

By Francis S. Stepka

Lewis Flight Propulsion Laboratory
Cleveland, Ohio

NATIONAL ADVISORY COMMITTEE
FOR AERONAUTICS

SEP 5 1958

WASHINGTON
September 4, 1958

[redacted]

NATIONAL ADVISORY COMMITTEE FOR AERONAUTICS

RESEARCH MEMORANDUM

COMPARISON OF CALCULATED AND EXPERIMENTAL TEMPERATURES AND COOLANT PRESSURE LOSSES FOR A CASCADE OF SMALL AIR-COOLED TURBINE ROTOR BLADES*

By Francis S. Stepka

SUMMARY

Average spanwise blade temperatures and cooling-air pressure losses through a small (1.4-in. span, 0.7-in. chord) air-cooled turbine blade were calculated and are compared with experimental nonrotating cascade data. Two methods of calculating the blade spanwise metal temperature distributions are presented. The method which considered the effect of the length-to-diameter ratio of the coolant passage on the blade-to-coolant heat-transfer coefficient and assumed constant coolant properties based on the coolant bulk temperature gave the best agreement with experimental data. The agreement obtained was within 3 percent at the midspan and tip regions of the blade. At the root region of the blade, the agreement was within 3 percent for coolant flows within the turbulent flow regime and within 10 percent for coolant flows in the laminar regime. The calculated and measured cooling-air pressure losses through the blade agreed within 5 percent.

Calculated spanwise blade temperatures for assumed turboprop engine operating conditions of 2000° F turbine-inlet gas temperature and flight conditions of 300 knots at a 30,000-foot altitude agreed well with those obtained by the extrapolation of correlated experimental data of a static cascade investigation of these blades.

INTRODUCTION

The cooling of small turbine blades, such as encountered in turboprop engines, can be much more difficult than cooling the larger blades of turbojet engines (refs. 1 and 2). In addition, the experimental data that have been obtained for small blades are meager. In order to provide information useful for the design of small air-cooled blades, this report will show the applicability of methods for analytically predicting the cooling-air pressure losses and the average temperatures at various spanwise positions of small turbine blades.

*Title, Unclassified.

Reference 2 presents a correlation of experimental blade temperature data that were obtained in a static cascade test facility over a range of gas temperatures and cooling airflow rates. It is indicated that the correlation parameters evolved permit the extrapolation of experimental blade temperature data to conditions other than test conditions. The applicability of analytical methods for determining blade temperatures and cooling-air pressure drops for these small blades in a manner similar to that employed for larger turbojet blades (ref. 3), however, was not known. This report, therefore, presents analytical methods for calculation of blade spanwise temperature distributions and cooling-air pressure drops and verifies the calculated results with the experimental blade temperature data used in reference 2 and with the experimental cooling-air pressure loss data presented herein. These analytical methods are applied to predict coolant-flow requirements, blade temperatures, and cooling-air pressure drops for an air-cooled blade configuration operating at an increased gas temperature and at typical flight conditions of a turboprop engine. In addition, these calculated blade temperatures are compared with those predicted by extrapolation of the correlated experimental data of reference 2.

The comparisons of the calculated and experimental nonrotating cascade data were made at total gas temperatures of 600°, 900°, and 1200° F and for three cooling airflow rates covering the range investigated in reference 2. The blade cooling-air inlet temperatures of the experimental data ranged from 150° to 493° F. The ratios of average blade metal to average blade cooling-air temperatures (°R) ranged from 1.18 to 1.45. The engine and flight conditions assumed for the calculations of blade cooling and pressure drop characteristics at high turbine-inlet gas temperature were: an engine with a compressor pressure ratio of 10.9, an airflow of 13.4 pounds per second, and a turbine-inlet gas temperature of 2000° F at a flight condition of 300 knots and an altitude of 30,000 feet.

SYMBOLS

A	flow area, sq ft
b	effective fin length, ft
C	constant
c_p	specific heat at constant pressure, Btu/(lb)(°F)
$D_{h,a}$	hydraulic diameter of coolant passage, 4A/(wetted perimeter), ft
$D_{h,g}$	hydraulic diameter of gas side of blade, l_g/π, ft

F	constant, function of blade transition ratio and Euler number
$F(\alpha)$	function of coolant passage aspect ratio
f	friction factor
g	acceleration due to gravity, ft/sec^2
ΔH	turbine work, Btu/lb
h	heat-transfer coefficient, Btu/(sec)(sq ft)($^\circ$F)
h_e	effective blade-to-coolant heat-transfer coefficient, Btu/(sec)(sq ft)($^\circ$F)
J	mechanical equivalent of heat, ft-lb/Btu
K	entrance loss coefficient
k	thermal conductivity, Btu/(sec)(ft)($^\circ$F)
L	length of blade or passage, ft
l	blade wall perimeter, ft
m	exponent, function of blade transition ratio and Euler number
N	number of fins
Nu	Nusselt number, $h_a D_{h,a}/k_a$ or $h_g D_{h,g}/k_g$
n	number of sections of equivalent fins
P	pressure, lb/sq ft
Pr	Prandtl number, $gc_p\mu/k$
R	gas constant, ft-lb/(lb)($^\circ$F)
$(\overline{Re})_a$	Reynolds number of coolant based on bulk temperature, $\frac{w_a D_{h,a}}{A_a \mu_a}$
$(Re)_{a,f}$	Reynolds number of coolant based on film temperature, $\frac{w_a D_{h,a}}{A_a \mu_{a,f}} \frac{T_a}{T_f}$

$(\overline{Re})_{g,B}$ average Reynolds number of gas based on blade temperature, $\frac{\bar{V}_g \bar{D}_{h,g} \bar{\rho}_{g,B}}{\bar{\mu}_{g,B}}$

r radius from center of rotation to center of blade increment, ft

s fin spacing, ft

T temperature, $^{\circ}R$

U peripheral velocity at hub of turbine rotor, ft/sec

V velocity, ft/sec

w weight-flow rate, lb/sec

Δx incremental blade or coolant passage length, ft

y coolant passage height, ft

z coolant passage width, ft

μ viscosity, (lb)(sec)/sq ft

ρ density, lb/cu ft

τ fin thickness, ft

ω angular velocity, radians/sec

Subscripts:

a cooling air or cooling-air side

B blade or blade metal

C compressor

e effective

f film temperature

g combustion gas or combustion-gas side

i blade inlet

in inside of coolant passage at entrance

o outlet

x condition at x feet above blade root

ζ index of summation

∞ fully established flow, cooling air

Superscripts:

' total conditions

$\bar{}$ average conditions for an incremental length

$\bar{\bar{}}$ average conditions for entire blade

DESCRIPTION OF BLADE AND PRESSURE DROP APPARATUS

The air-cooled turbine rotor blade configuration selected for the analytical determination of blade temperature distributions and cooling-air pressure losses is the same as that of the blade for which experimental temperature data were obtained in the investigation of reference 2. The blade, referred to herein as the cast finned blade, has a span and chord of approximately 1.4 and 0.7 inch, respectively. Cross-sectional views of the tip, midspan, and root regions of the blade are shown in figure 1. The external blade size and airfoil shape are the same as those employed in the first-stage turbine rotor of a current uncooled commercial turboprop engine. As a matter of interest, the cooled blade was fabricated from two parts as shown in figures 1 and 2(a): one part includes an integrally cast base, the airfoil suction surface, and the cooling fins; and the other a formed sheet-metal pressure surface. The formed sheet-metal shell was brazed in the recesses at the leading- and trailing-edge regions of the blades to several of the cast cooling fins (fig. 1) and to the base in the root region. A photograph of a completed blade is shown in figure 2(b). A more detailed description of the blade and its fabrication is presented in reference 2.

A schematic sketch of the apparatus and instrumentation used to obtain the cooling-air entrance loss coefficient and the over-all cooling-air pressure losses for the cast finned blade is shown in figure 3. The test-blade base was brazed to a sheet-metal duct through which laboratory compressed air was supplied to the blade. The duct used was intended to simulate a blade entrance which might be expected when cooling air is supplied to blades in a turbine rotor. In addition to the instrumentation shown in figure 3, a thermocouple to measure the total cooling-air temperature was located in a plenum chamber upstream of the cooling-air entrance duct. The static pressure at the blade tip was the measured ambient pressure.

ANALYSIS AND PROCEDURE

The blade metal and cooling-air temperatures at various spanwise positions were obtained from an iterative procedure which utilized heat balances between gas and coolant at the spanwise position under consideration. To solve these heat balances it was necessary to determine the gas-to-blade and blade-to-coolant heat-transfer coefficients and to account for the effectiveness of coolant passage fins.

Calculations of Gas-to-Blade Heat-Transfer Coefficient

The gas-to-blade heat-transfer coefficient $\bar{h}_g$ used in the analysis is an average coefficient for the blade and was obtained from the correlation equation of reference 4:

$$(\overline{Nu})_g = F\left[(\overline{Re})_{g,B}\right]^m\left[(\overline{Pr})_{g,B}\right]^{1/3} \tag{1}$$

where $F = 0.092$ and $m = 0.070$. The values of F and m, which were obtained from reference 5, are the average values of ten rotor blade profiles including both impulse and reaction blades. The gas properties used were evaluated at the average metal temperature of the entire blade $\bar{T}_B$. Equation (1) can be expressed as

$$\bar{h}_g = 0.092\,\frac{\bar{k}_{g,B}}{D_{h,g}}\left[(\overline{Re})_{g,B}\right]^{0.7}\left[(\overline{Pr})_{g,B}\right]^{1/3} \tag{2}$$

The average gas-to-blade heat-transfer coefficient as determined from equation (2) was used at each spanwise location considered in the calculations.

Calculations of Blade-to-Coolant Heat-Transfer Coefficient

Two methods of calculating blade-to-coolant heat-transfer coefficients were used in order to determine which best predicted the experimental blade spanwise temperature distribution. One of the methods used was the same as that used to predict temperatures of turbine blades for turbojet engines (refs. 3 and 6) wherein the flow through the blades was assumed fully developed. Reference 6 presents the equations for determining the blade-to-coolant heat-transfer coefficients, which in the notation of this report for flow in the assumed turbulent (Reynolds number greater than 6000) and laminar (Reynolds number less than 2300) flow regions, respectively, are

$$(Nu)_{a,\infty} = 0.023\left[(Re)_{a,f}\right]^{0.8}\left[(Pr)_{a,f}\right]^{0.4} \tag{3}$$

and

$$(Nu)_{a,\infty} = F(\alpha) \tag{4}$$

The term $F(\alpha)$ is a function of aspect ratio of the coolant passage, which is the ratio of the height to the width of the coolant passage (e.g., y/z in fig. 1). Values of $F(\alpha)$ are given for various aspect ratios in reference 7. The aspect ratio for the finned portion of the cast finned blade was approximately 3 and that for the hollow-tip region was approximately 8. The corresponding values of $F(\alpha)$ as obtained from reference 7 were 4.77 and 6.5, respectively. The coolant properties along the blade span were evaluated at local film temperatures. The film temperature was assumed to be the arithmetic average of the blade metal and coolant temperatures at each spanwise position considered.

The effectiveness of coolant passage fins was accounted for by replacing the coolant passage geometry (for the region of the blade where the fins were located) by one of equivalent fins (ref. 3) and by using the equation for the effective blade-to-coolant heat-transfer coefficient (eq. (6), ref. 3). This equation expressed in the notation of this report is

$$h_e = \sum_{\zeta=1}^{n} \frac{h_a}{N_\zeta(s_\zeta + \tau_\zeta)} \left[\sum_{\zeta=1}^{n} \frac{N_\zeta 2b_\zeta \tanh\left(b\sqrt{2h_a/\bar{k}_B\tau}\right)_\zeta}{\left(b\sqrt{2h_a/\bar{k}_B\tau}\right)_\zeta} + \sum_{\zeta=1}^{n} N_\zeta s_\zeta \right] \tag{5}$$

The analyses of references 3 and 6 assumed fully developed flow through the blade. It was assumed that entrance effects on the blade-to-coolant heat-transfer coefficient would be small because of the large length-to-diameter ratio of the turbojet blades ($L/\bar{D}_{h,a} = 70$). The length-to-diameter ratio of the small turbine blade ($L/\bar{D}_{h,a} = 38$) considered herein, however, was small compared with that of the blades for turbojet engines. The second method used to determine the blade-to-coolant heat-transfer coefficients, therefore, considered the coolant passage entrance effects, that is, the $L/\bar{D}_{h,a}$ effect.

The blade-to-coolant Nusselt number used for the second method of calculating blade temperatures was an average for the entire blade and was obtained from correlation equations for flow through rectangular tubes (ref. 7). In the notation of this report, the equations for turbulent and laminar flow are, respectively,

$$(\bar{Nu})_a = 0.02 \left[(\bar{Re})_a\right]^{0.8} (\bar{T}_a/\bar{T}_B)^{0.4} \left[(\bar{Pr})_a\right]^{1/3} \left(1 + \frac{3.8}{L/\bar{D}_{h,a}}\right) \tag{6}$$

$$(\overline{Nu})_a = F(\alpha)\left[1 + \frac{C(\overline{Re})_a(\overline{Pr})_a}{L/D_{h,a}}\right] \quad (7)$$

The values of the constant C and the term $F(\alpha)$ in equation (7) are dependent on the aspect ratio of the coolant passages. The average aspect ratio of the coolant passages, when neglecting the small length of blade near the tip which did not have fins in the passage, was about 3. The values of C and $F(\alpha)$ at an aspect ratio of 3 as obtained from reference 7 were 0.009 and 4.77, respectively. The coolant properties used in equations (6) and (7) were based on the bulk temperature of the coolant. The bulk temperature was the arithmetic average of the air temperatures of the blade inlet and exit. Because of the variation of the hydraulic diameter of the coolant passage along the blade span and in order to consider this variation in the coolant passage diameter, the blade-to-coolant heat-transfer coefficient h_a at a given spanwise position was defined as

$$h_a = \frac{(\overline{Nu})_a \bar{k}_a}{D_{h,a}} \quad (8)$$

The effectiveness of the fins in the coolant passage was accounted for in the same manner as discussed previously and by the use of equation (5). The Nusselt numbers in the assumed transition flow region (Reynolds numbers between 2300 to 6000) were obtained by assuming a straight-line relation of Nusselt number with Reynolds number in this range and by using Nusselt numbers calculated from equation (3) or (6) as the turbulent-flow end point and from equation (4) or (7) as the laminar-flow end point.

Calculation of Spanwise Blade and Cooling-Air Temperatures

In the analysis the blade span was divided into four approximately equal increments. The geometry parameters were obtained by cutting the test blades after completion of the investigation of reference 2 at the four spanwise locations considered herein and making photographs of the cross sections at a magnification of 10. The calculation of blade temperatures for comparison with the experimental data of reference 2 was made for the three cascade gas temperatures of 600°, 900°, and 1200° F considered in that investigation and for three cooling airflow rates, which represented the extremes and the middle values of the rates that were supplied to the test blades at each gas temperature. The analysis was made by using the average velocities of the combustion gas relative to the blades, average combustion-gas static pressures, effective gas spanwise temperature distributions, and the blade cooling-air inlet temperatures obtained in the experimental investigation of reference 2.

The iterative procedure for calculating the spanwise blade and cooling-air temperatures was first to assume an average blade temperature $\bar{T}_B$, which together with the average velocity of the gas relative to the blade, the average hydraulic diameter of the gas side of the blade, and the gas properties evaluated at $\bar{T}_B$ permitted calculation of the gas-to-blade heat-transfer coefficient by use of equation (2). By assuming an average chordwise blade temperature $T_{B,x}$ for each spanwise position and by specifying the effective gas temperature distribution, the geometry of the blade, the coolant-flow rate, and the coolant temperature at the root, the coolant temperature at other than the root position could be obtained. This was done by adding the coolant temperature rise for each increment to the coolant temperature at the beginning of the increment. The incremental temperature rise of the coolant $\Delta T_a'$ was obtained from the following heat balance:

$$\bar{h}_g \bar{l}_g (\bar{T}_{g,e} - \bar{T}_B)\Delta x + \frac{w_g \omega^2 r \, \Delta x}{gJ} = w_a c_{p,a} \, \Delta T_a' \tag{9}$$

or

$$\Delta T_a' = \frac{\bar{h}_g \bar{l}_g \, \Delta x}{w_a c_{p,a}} (\bar{T}_{g,e} - \bar{T}_B) + \frac{\omega^2 r \, \Delta x}{gJ c_{p,a}} \tag{10}$$

For calculation of blade temperature of a nonrotating blade the last term of equation (10), the air temperature rise due to the pumping work done on the air over the increment, is zero so that

$$\Delta T_a' = \frac{\bar{h}_g \bar{l}_g \, \Delta x}{w_a c_{p,a}} (\bar{T}_{g,e} - \bar{T}_B) \tag{11}$$

The values of $\bar{T}_{g,e}$ and $\bar{T}_B$ in equations (9) to (11) are the arithmetic average of the temperatures at the beginning and end of an increment. The effective blade-to-coolant heat-transfer coefficient at each span position was then calculated by use of equations (3) or (4) and (5) when the coolant flow was considered to be fully developed. The assumed average chordwise blade temperature $T_{B,x}$ at each span location was then checked by solving the following heat balance equation:

$$\bar{h}_g l_g (T_{g,e,x} - T_{B,x}) = h_e l_a (T_{B,x} - T_{a,x}') \tag{12}$$

where $T_{g,e,x}$ and $T_{a,x}'$ are the effective gas temperature and the total cooling-air temperature relative to the blade. The latter temperature is approximately equal to the effective air temperature for subsonic Mach

numbers. The assumed average blade temperature $\overline{T}_B$ was checked with the integrated average of the calculated spanwise blade temperature distribution. If agreement was not obtained, the process was repeated.

In the calculations which accounted for the blade entrance effect on the heat transfer to the coolant, the blade-to-coolant heat-transfer coefficient was obtained by use of equations (6) or (7), (8), and (5) after a coolant bulk temperature $\overline{T}_a$ was assumed. An iterative procedure was then used to calculate the spanwise blade and coolant temperature by use of equations (11) and (12). The assumed average blade temperature $\overline{T}_B$ and the assumed coolant bulk temperature $\overline{T}_a$ were checked with integrated averages of the calculated spanwise distributions, and, if agreement was not obtained, the process was repeated.

Calculation of Blade Cooling-Air Pressure Loss

The cooling-air pressure loss through the blade airfoil, which was divided into four approximately equal incremental lengths, was calculated by the method of reference 8. The average friction factor $\overline{f}$ used in the calculations was determined by the use of the following correlation equations for laminar and turbulent flows, respectively, obtained from reference 7 and given in the notation of this report:

$$\frac{\left[\overline{f(\mathrm{Re})}_a\right]}{\left[f(\mathrm{Re})\right]_\infty} = 1 + \frac{0.005(\overline{\mathrm{Re}})_a}{L/\overline{D}_{h,a}} \tag{13}$$

and

$$\overline{f} = 0.040(\overline{\mathrm{Re}})_a^{-0.2}\left(1 + \frac{10}{L/\overline{D}_{h,a}}\right) \tag{14}$$

The term $\left[f(\mathrm{Re})\right]_\infty$ is a function of passage aspect ratio. For a coolant passage aspect ratio of 3, the value of $\left[f(\mathrm{Re})\right]_\infty$ as obtained from reference 7 was 17.1. Inasmuch as the previous equations and the method of reference 8 permit calculation of the pressure loss through the airfoil only, the pressure loss at the blade entrance due to a sudden contraction of the flow passage is required in order to calculate the over-all pressure loss. The pressure drop across the blade entrance can be determined by solving the following equation from reference 9, which is presented in the nomenclature of this report:

$$\frac{P'_{a,i} - P'_{a,in}}{P_{a,in}} = K\left(\frac{w_a^2 T_{a,in}}{A_a^2 p^2_{a,in}}\right)\frac{R}{2g} \tag{15}$$

Because of the lack of information on entrance loss coefficients for flow conditions and geometries which would duplicate those at the entrance to the blade, an experimentally determined value of the coefficient K for the test blade was used. In the determination of cooling-air pressure loss through the blade for comparison with experimental data, the tip static pressure and the cooling-air temperature of the experimental investigation were used.

Experimental Determination of Blade Cooling-Air Pressure Loss

The experimental pressure losses for the cast finned blade were obtained at room temperatures and pressures with the apparatus described previously. The cooling-air pressure losses were obtained over a range of coolant-flow rates from 7×10^{-4} to 8.6×10^{-3} pound per second. The range covered the lowest flow that could be measured in this installation to approximately choked flow in the blade. The cooling-air inlet temperature was constant for the investigation and was approximately 80° F. The over-all pressure loss was the measured difference between the inlet total-pressure probe reading and the tip static pressure, which was assumed to be ambient pressure. The blade entrance loss coefficient K was obtained by the method described in reference 9. This method requires the use of the experimental data in the parameter at the left side of equation (15) and in the parameter in parentheses on the right of the same equation. The first parameter is then plotted as the ordinate against the second parameter on log-log paper for each data point. From this plot the value of K may be determined.

RESULTS AND DISCUSSION

Comparison of Calculated and Experimental Blade Spanwise Temperature Distributions

The spanwise blade metal temperature distributions for the 1200° F gas temperature were calculated using the two methods of calculation already described. One assumed fully developed coolant flow, based the coolant properties on film temperature, and considered the variation of properties with film temperature along the blade span. The other method considered the effect of the length-to-hydraulic-diameter ratio of the coolant passage on the blade-to-coolant heat-transfer coefficient and assumed constant coolant properties based on the coolant bulk temperature. The calculated spanwise blade temperature distributions for three coolant-flow rates at an inlet total gas temperature of approximately 1200° F are presented in figure 4 together with experimentally obtained data points at the root, midspan, and tip regions of the blade. The experimental data

points used were those used in reference 2 and were the average of six thermocouple readings around the periphery of the blade at each of the three span locations. The results indicate that, although both methods of calculating the spanwise blade metal temperatures agreed reasonably well with experimental data, better agreement was obtained using the method involving equations (6) and (7) which considered the length-to-diameter ratio ($L/\overline{D}_{h,a}$ = 38) of the coolant passage and assumed constant coolant properties. The agreement of the temperatures calculated by this method and the experimental data at the midspan and tip regions of the blade was within 3 percent. At the root region the agreement was within 3 percent for the two turbulent-flow runs and about 7 percent for the laminar-flow run. Inasmuch as equations (6) and (7) (used to evaluate the blade-to-coolant heat-transfer coefficient) are dependent on the length-to-diameter ratio $L/\overline{D}_{h,a}$ of the coolant passage, calculations were also made to determine to what extent the agreement between calculated and experimental data at the root region might be improved by considering the length-to-diameter ratio for a length of blade a short distance from the root. The distance from the root (approx. 0.56 in.) for this calculation was determined for a length-to-diameter ratio of 20, which was the lower limit for which equations (6) and (7) were experimentally verified as valid in reference 7. The blade spanwise metal temperature distributions obtained from these calculations are also shown in figure 4. The improvement in agreement with experimental data was small as compared with the data which were calculated by considering the full length of blade ($L/\overline{D}_{h,a}$ = 38). Since the improvement was small, the calculation method which assumed constant coolant properties and determined the blade-to-coolant heat-transfer coefficient by use of equations (6) and (7) for an $L/\overline{D}_{h,a}$ of 38 was used to determine the spanwise blade temperatures for the 600° and 900° F gas temperature runs as well as for an elevated temperature application, which is discussed in a later section. A plot of the average blade temperatures calculated by this method against the measured average temperatures at the root, midspan, and tip regions for all three inlet gas temperatures and over the entire range of coolant flows of the investigation of reference 2 is shown in figure 5. The agreement of the temperatures about a line representing 100-percent agreement is good. The maximum deviation at the tip and midspan regions was less than 3 percent. At the root region the agreement was within 3 percent for coolant flows in the turbulent regime and within 10 percent for coolant flow in the laminar regime.

Comparison of Calculated and Experimental Cooling-Air Pressure Loss

The calculated cooling-air pressure loss through the cast finned blade for a range of coolant flows is shown in figure 6 along with experimental data. The agreement between the calculated and experimental data was within 5 percent.

The cooling-air pressure loss due to contraction at the blade entrance was found to be a small part of the total cooling-air pressure loss of the blade. The cooling-air pressure loss at the blade entrance was 1 to 6 percent of the over-all pressure loss for cooling airflows of 0.004 and 0.0088 pound per second, respectively. The experimental entrance loss coefficient K was 0.37.

Blade Temperature and Pressure Losses at Elevated Temperatures

In view of the good agreement between the calculated and experimental static cascade data, the blade temperatures and cooling-air pressure losses for the cast finned blade configuration were calculated by assuming operation in a typical turboprop engine at an inlet gas temperature of 2000° F and flight conditions of 300 knots at a 30,000-foot altitude. The conditions assumed for the engine are as follows:

Compressor-inlet pressure recovery, percent	100
Compressor pressure ratio	10.9
Compressor efficiency	0.77
Compressor airflow, lb/sec	13.4
Combustor pressure loss ratio	0.95
Turbine efficiency	0.85
Number of turbine stages	4
Turbine rotative speed, rpm	13,820
Turbine work parameter, $gJ\,\Delta H/U^2$, last stage	2.5
Turbine work parameter of first three stages	Assumed equal (calculated to be 2.9)
Exhaust-nozzle pressure ratio	0.92

The gas-flow conditions relative to the first-stage turbine rotor blades were determined from the assumed engine conditions. The spanwise effective gas temperature distribution relative to the rotor blades for an average inlet total temperature of 2000° F was assumed similar in shape to that obtained in the experimental static cascade investigation of reference 2 and is shown in figure 7. This shape of the effective gas temperature profile was assumed in order to permit comparison of the extrapolated data of reference 2 with these calculated results on the same basis. The shape of the profile assumed is also similar to that which might be expected in an engine. The static pressure at the blade tips, used for the calculations of the blade pressure losses, was the arithmetic average of the calculated tip static gas pressures across the rotor stage. The blade entrance cooling-air temperature was assumed to be 623° F (calculated compressor-exit bleed temperature plus an assumed 100° F rise in the air temperature as it is ducted from the compressor to the entrance of the blades).

Cooled blade temperatures. - The calculated spanwise temperature distribution of the first-stage turbine rotor blades and the blade coolant temperature rise for coolant-flow ratios (ratio of cooling-air to combustion-gas flow) of 0.015, 0.02, and 0.03 are presented in figure 7. Also shown in the figure is the spanwise blade temperature distribution at a coolant-flow ratio of 0.015 obtained by extrapolation of the correlated experimental data of reference 2 by the method presented in reference 2. The agreement between the calculated temperature distribution and that obtained by extrapolation of the data of reference 2 was within 2 percent above the midspan region of the blade and within 10 percent at 3/16 inch above the blade root. This agreement is similar to that obtained previously when calculated blade temperature distributions were compared to the experimental blade temperature data that were used in reference 2. This agreement might be expected because the equations used to obtain the correlation parameters in reference 2 are the same as those used herein for the calculation of blade temperatures.

In order to determine the critical region of the blades at the conditions assumed, an allowable blade spanwise temperature distribution curve was obtained. This curve was tangent to the curve of the calculated blade temperature distribution at a coolant-flow ratio of 0.015 (fig. 7). The point of tangency of the two curves, which is approximately at the midspan of the blade, indicates the critical region of the blade. The midspan of the blade is also the spanwise region of the blade where the calculated blade metal temperatures agreed well with experimental data. The allowable spanwise temperature distribution curve shown in figure 7 was based on a stress ratio factor (ratio of allowable stress-rupture strength to calculated centrifugal stress) of 2.8 and a life of 1000 hours for the high-temperature alloy HS-31. The stress ratio factor of 2.8 appears adequate based on values of this factor obtained in references 10 to 12 for blades in a turbojet engine. Reference 10 showed that, for one type of blade configuration made of alloy 17-22A(S), the required stress ratio factor was 2.3. Values of stress ratio factors between 1.2 and 1.5 were obtained in references 11 and 12 for blade configurations made of alloy HS-31. The blades in these two references were either investigated uncooled or with small quantities of cooling air with the result that the peripheral temperature gradients and the resulting thermal stresses were small. The stress ratio factors obtained were nevertheless indicative of the margin of safety required for blade configurations under engine test conditions. If it is assumed that the stress ratio factor of 2.8 is sufficient to account for such factors as vibratory stress, thermal stresses, metallurgical changes with time, and so forth, the calculations indicate that the cast finned blades (based on stress-rupture strength of HS-31) will require a coolant-flow ratio of approximately 0.015 for a blade life on the order of 1000 hours at the assumed engine and flight conditions.

Cooling-air pressure losses. - With the cooling-air spanwise temperature distribution and the tip static pressure, the pressure loss through the blade $P'_{a,i} - P_{a,o}$ was determined for a range of coolant-flow ratios from 0.015 to 0.030. The results are shown in figure 8(a). The calculations indicate that the cooling-air pressure losses through the first-stage turbine rotor blade are small. This is primarily due to the rise in cooling-air pressure within the blade due to the pumping effect of the high rotative speeds. At the coolant-flow ratio of 0.015, the pressure rise due to pumping effects was larger than the pressure losses due to heat transfer and friction, with the result that a small pressure rise (0.4 in. Hg) was obtained. Figure 8(b) shows a plot of the ratio of pressure required at the blade base to compressor-exit pressure for a range of coolant-flow ratios. At a coolant-flow ratio of 0.015 the required pressure at the blade entrance is only about 61 percent of the compressor-exit pressure. The calculations further indicate that higher coolant-flow ratios can be supplied to the blade without the blade being pressure limited. For example, at a coolant-flow ratio of 0.03, the ratio of $P'_{a,i}/P'_{C,o}$ is only about 0.67. The low ratios of the required cooling-air pressure at the blade entrance to compressor-exit pressure indicate that relatively large losses in the ducting from the compressor exit to the blade cooling-air entrance can be tolerated. Another possibility, since these losses are small, is to bleed the engine compressor at points ahead of the last stage and thereby obtain slightly lower power reductions and specific-fuel-consumption increases than with compressor-discharge bleed (ref. 13). Bleeding the compressor ahead of the last stage would also provide lower temperature cooling air to the blade and thus result in lower blade temperatures or permit further reduction of cooling air-flow to the blades.

SUMMARY OF RESULTS

The results of an analytical investigation to determine the blade temperature distributions and cooling-air pressure losses for a small air-cooled turbine blade of a turboprop engine are as follows:

1. The calculated spanwise blade metal temperatures agreed well with static cascade experimental data.

2. Two methods of calculating blade temperatures were employed. One method assumed fully developed coolant flow, based the coolant properties on film temperature, and considered the variation of properties with film temperature along the span of the blade. The other method considered the effect of the length-to-diameter ratio of the coolant passage on the blade-to-coolant heat-transfer coefficient and assumed constant coolant properties based on the coolant bulk temperature. The use of this latter method gave the best agreement with experimental data. The agreement obtained

was within 3 percent at the midspan and tip regions of the blade. At the root region of the blade the agreement was within 3 percent for coolant flows within the turbulent flow regime and within 10 percent for coolant flows in the laminar regime.

3. Calculated cooling-air pressure losses within the blades agreed within 5 percent with experimental data.

4. Calculated spanwise blade metal temperature distributions of the cast finned blade for assumed operation at a turbine-inlet gas temperature of 2000° F in a typical turboprop engine at flight conditions of 300 knots and an altitude of 30,000 feet agreed well with those obtained by the extrapolation of the correlated experimental data of a static cascade investigation with these blades. The agreement was within 2 percent above the midspan region of the blade and within 10 percent at a distance 3/16 inch above the blade root.

5. Calculations for the assumed engine and flight conditions also indicated that the first-stage rotor blades of the cast finned configuration (based on stress-rupture strength of HS-31) will require a coolant-flow ratio of about 0.015 for a blade life on the order of 1000 hours. The calculated cooling-air pressure required at the entrance to the first-stage rotor blades for these conditions was only about 61 percent of the compressor-exit pressure.

Lewis Flight Propulsion Laboratory
National Advisory Committee for Aeronautics
Cleveland, Ohio, May 27, 1958

REFERENCES

1. Esgar, Jack B., Schum, Eugene F., and Curren, Arthur N.: Effect of Chord Size on Weight and Cooling Characteristics of Air-Cooled Turbine Blades. NACA TN 3923, 1957.

2. Stepka, Francis S., Richards, Hadley T., and Hickel, Robert O.: Cascade Investigation of Cooling Characteristics of a Cast-Finned Air-Cooled Turbine Blade for Use in a Turboprop Engine. NACA RM E57D19, 1957.

3. Ziemer, Robert R., and Slone, Henry O.: Analytical Procedures for Rapid Selection of Coolant Passage Configurations for Air-Cooled Turbine Rotor Blades and for Evaluation of Heat-Transfer, Strength, and Pressure-Loss Characteristics. NACA RM E52G18, 1952.

4. Brown, W. Byron, and Donoughe, Patrick L.: Extension of Boundary-Layer Heat-Transfer Theory to Cooled Turbine Blades. NACA RM E50F02, 1950.

5. Donoughe, Patrick L.: Outside Heat Transfer of Bodies in Flow - A Comparison of Theory and Experiment. M.S. Thesis, Case Inst. Tech., 1951.

6. Slone, Henry O., Hubbartt, James E., and Arne, Vernon L.: Method of Designing Corrugated Surfaces Having Maximum Cooling Effectiveness Within Pressure-Drop Limitations for Application to Cooled Turbine Blades. NACA RM E54H20, 1954.

7. Kays, W. M., and Clark, S. H.: A Summary of Basic Heat Transfer and Flow Friction Design Data for Plain Plate-Fin Heat Exchanger Surfaces. Tech. Rep. No. 17, Dept. Mech. Eng., Stanford Univ., Aug. 15, 1953. (Contract N6- 251 for Office Naval Res.)

8. Hubbartt, James E., Slone, Henry O., and Arne, Vernon L.: Method for Rapid Determination of Pressure Change for One-Dimensional Flow with Heat Transfer, Friction, Rotation, and Area Change. NACA TN 3150, 1954.

9. Brown, W. Byron, and Slone, Henry O.: Pressure Drop in Coolant Passages of Two Air-Cooled Turbine-Blade Configurations. NACA RM E52D01, 1952.

10. Stepka, Francis S., Bear, H. Robert, and Clure, John L.: Experimental Investigation of Air-Cooled Turbine Blades in Turbojet Engine. XIV - Endurance Evaluation of Shell-Supported Turbine Rotor Blades Made of Timken 17-22A(S) Steel. NACA RM E54F23a, 1954.

11. Schum, Eugene F., Stepka, Francis S., and Oldrieve, Robert E.: Fabrication and Endurance of Air-Cooled Strut-Supported Turbine Blades with Struts Cast of X-40 Alloy. NACA RM E56A12, 1956.

12. Freche, John C., and Schum, Eugene F.: Cooling Performance and Structural Reliability of a Modified Corrugated-Insert Air-Cooled Turbine Blade with an Integrally Cast Shell and Base. NACA RM E56K09, 1957.

13. Esgar, Jack B., and Ziemer, Robert R.: Effect of Turbine Cooling with Compressor Air Bleed on Gas-Turbine Engine Performance. NACA RM E54L20, 1955.

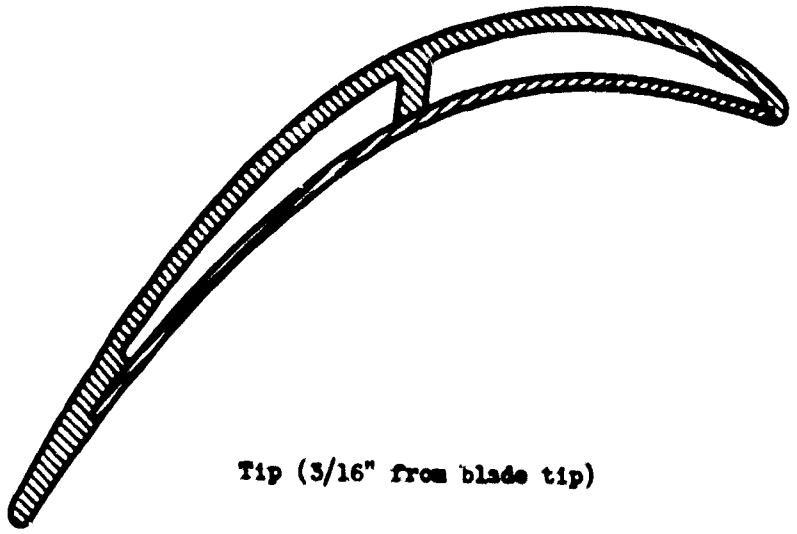

Tip (3/16" from blade tip)

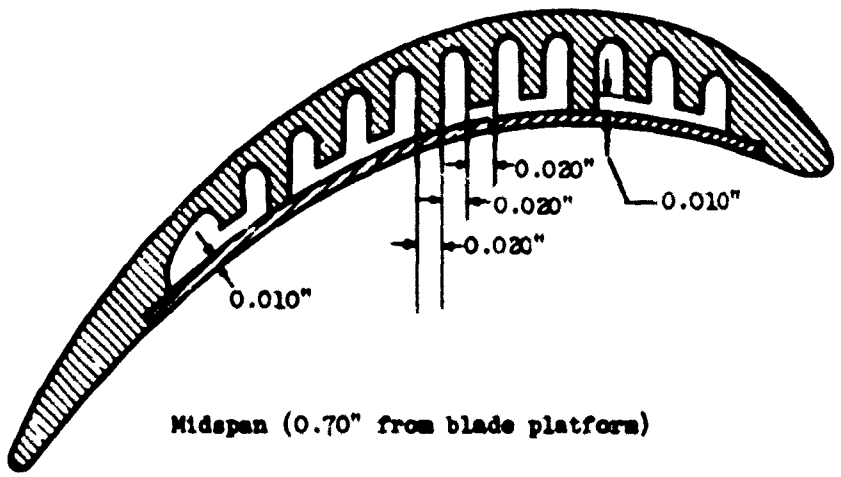

Midspan (0.70" from blade platform)

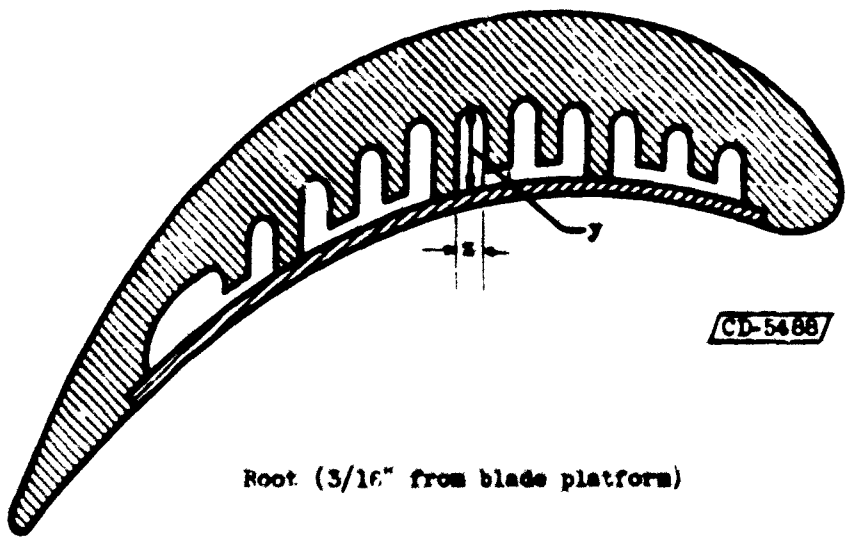

Root (3/16" from blade platform)

Figure 1. - Cross-sectional views of cast finned air cooled turbine blade (1.4-in. span and 0.7-in. chord) at approximately the root, midspan, and tip locations.

Sheet-metal shell (pressure surface)

Integrally cast base, suction surface, and cooling fins

(a) Blade before assembly.

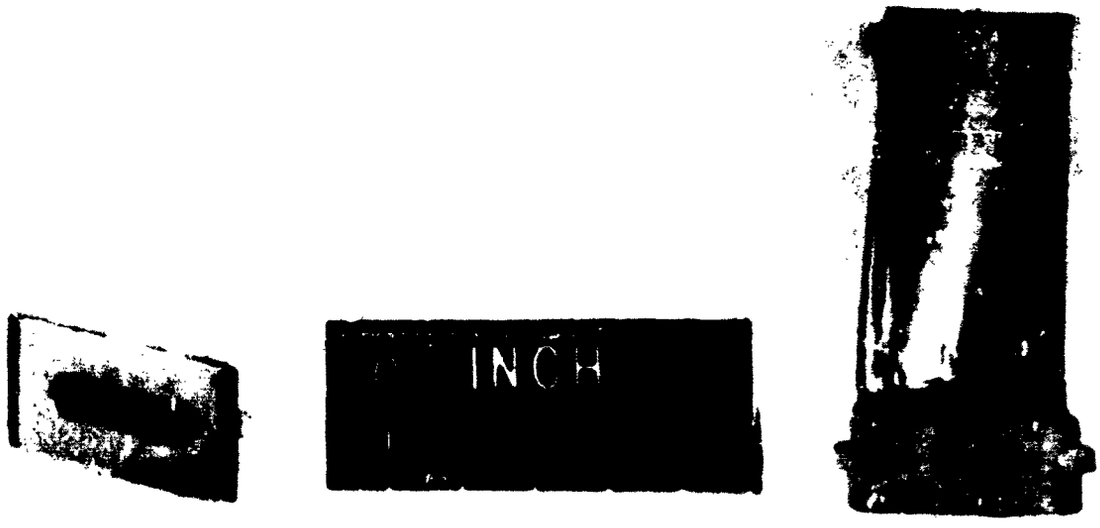

Bottom view

Side view

C-44787

(b) Assembled blade.

Figure 2. - Blade components before and after assembly.

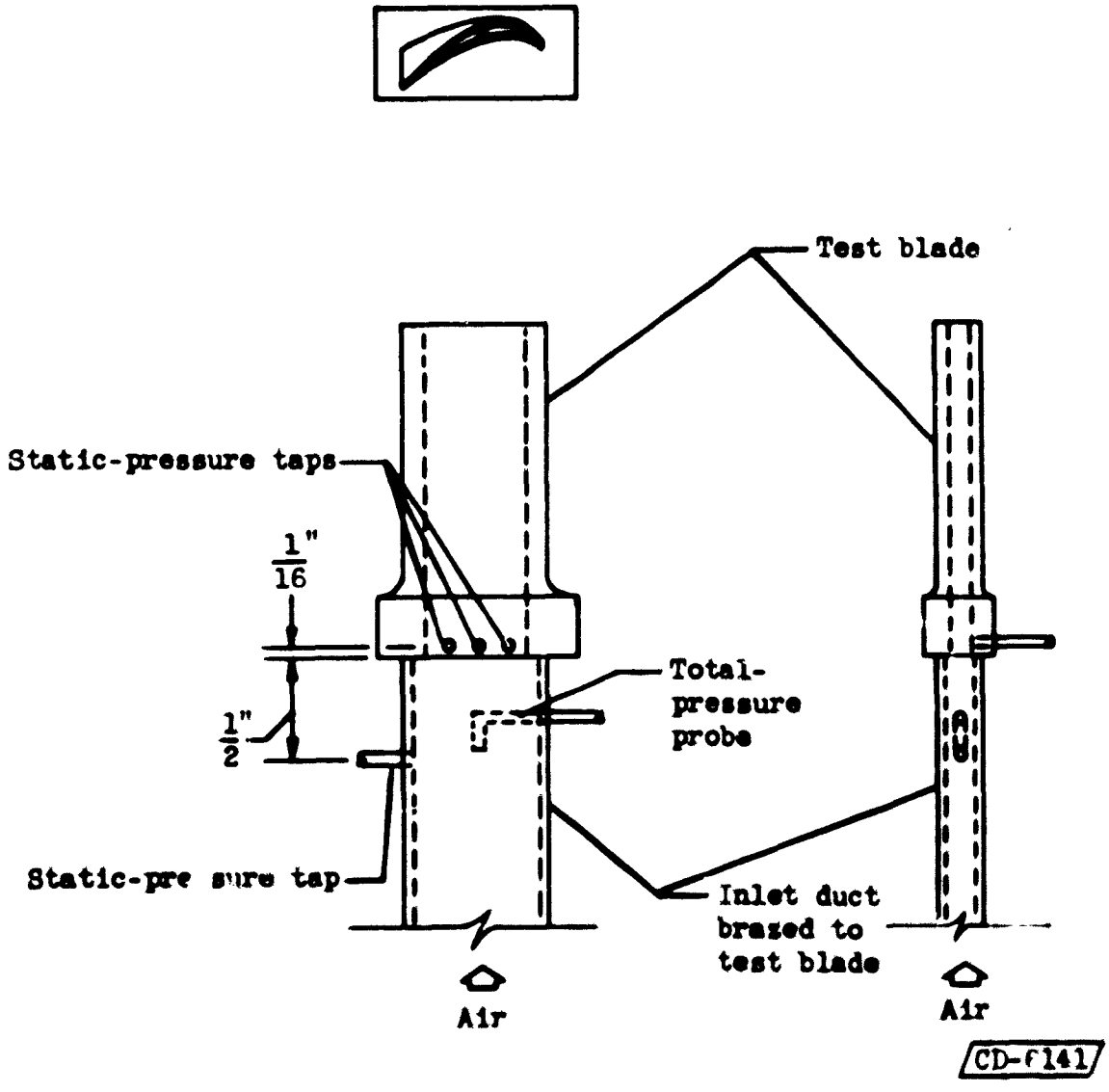

Figure 3. - Schematic sketch of apparatus and instrumentation for obtaining cooling-air pressure drop through cast finned air-cooled turbine blade.

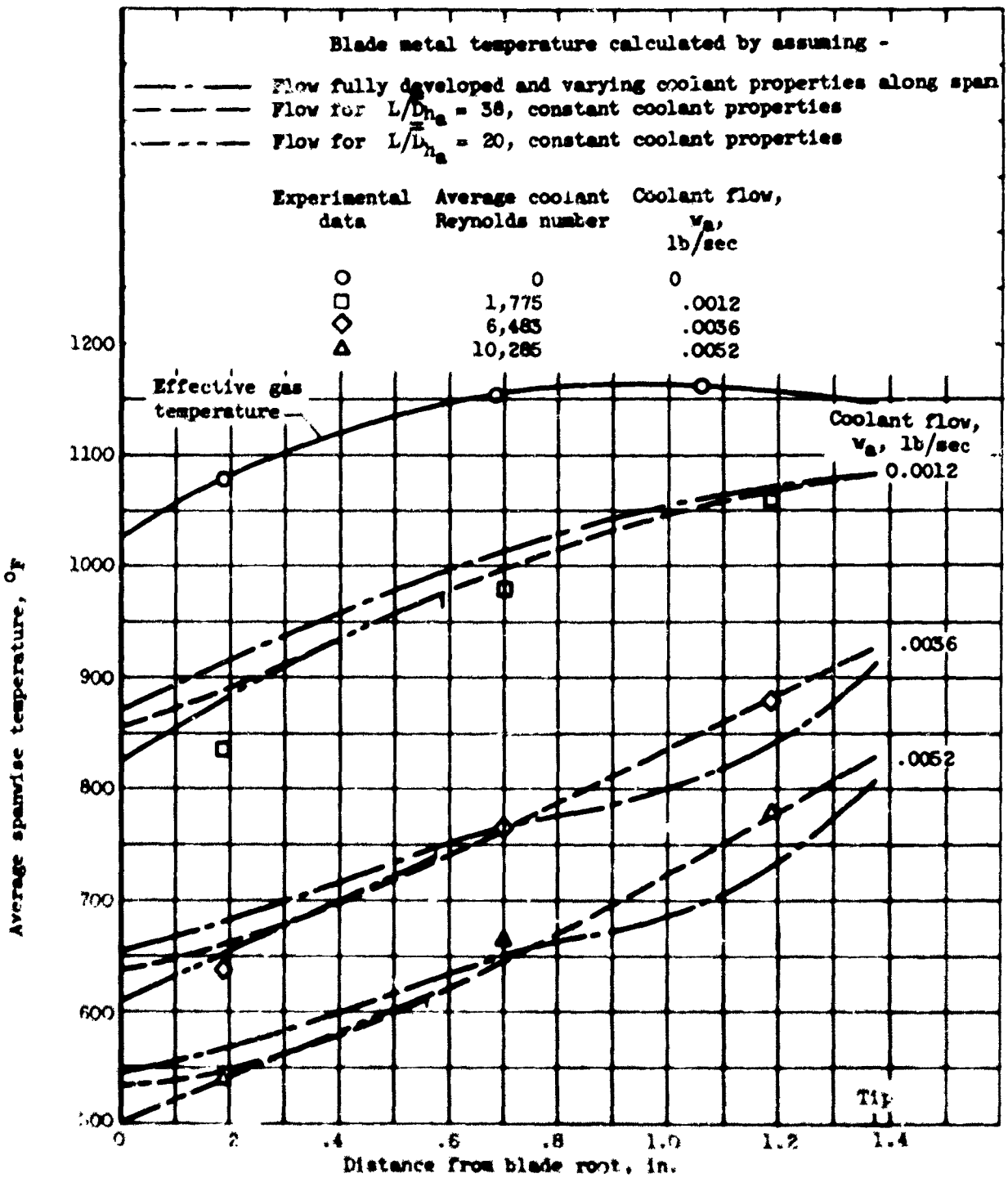

Figure 4. - Comparison of calculated average blade temperatures with average experimental cascade temperatures at various spanwise positions. Inlet gas temperature, approximately 1200° F; coolant-flow range, 0 to 0.007 pound per second.

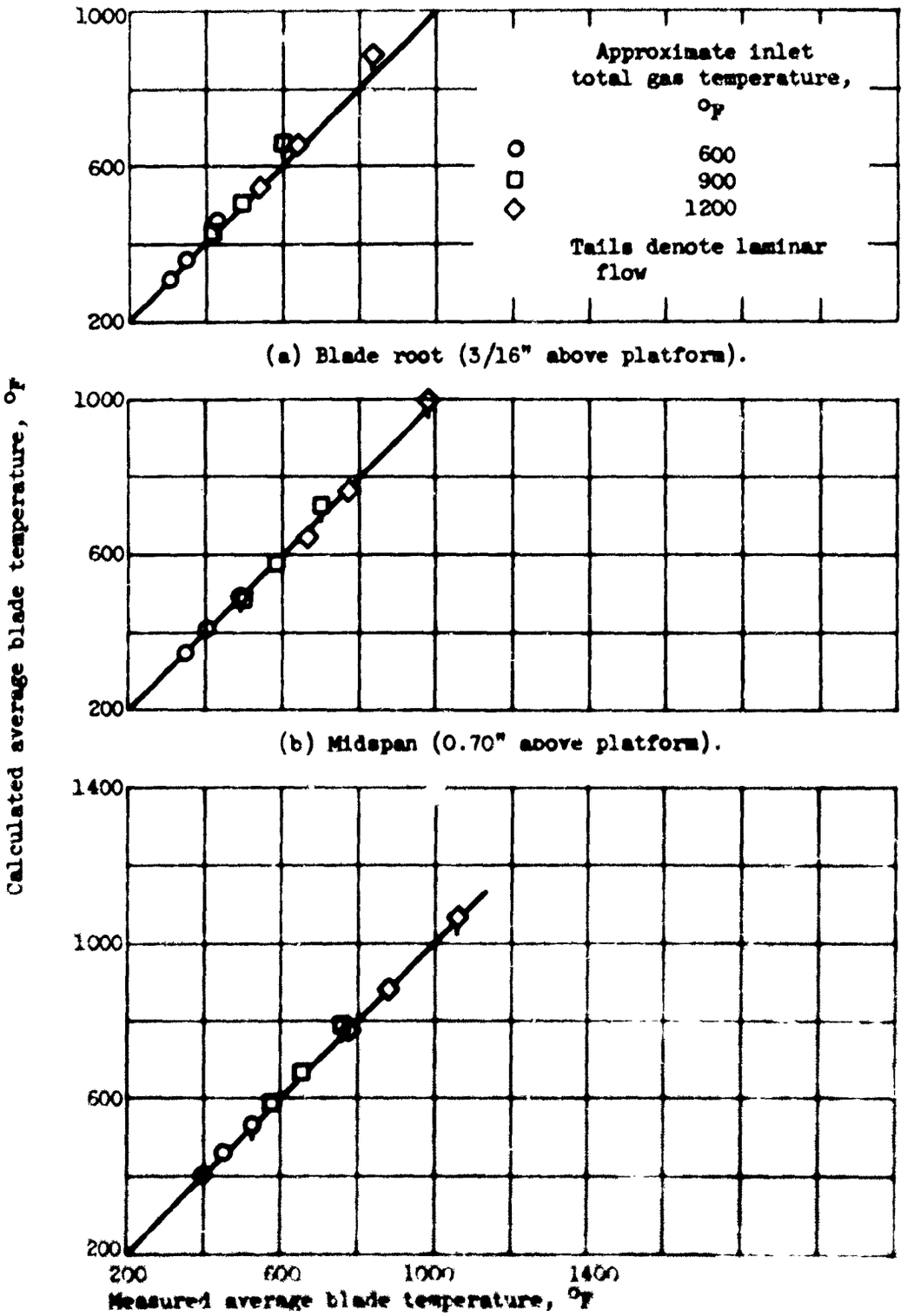

Figure 5. - Comparison between calculated average and measured average cascade blade metal temperatures at several spanwise stations for range of inlet gas temperatures and coolant flows.

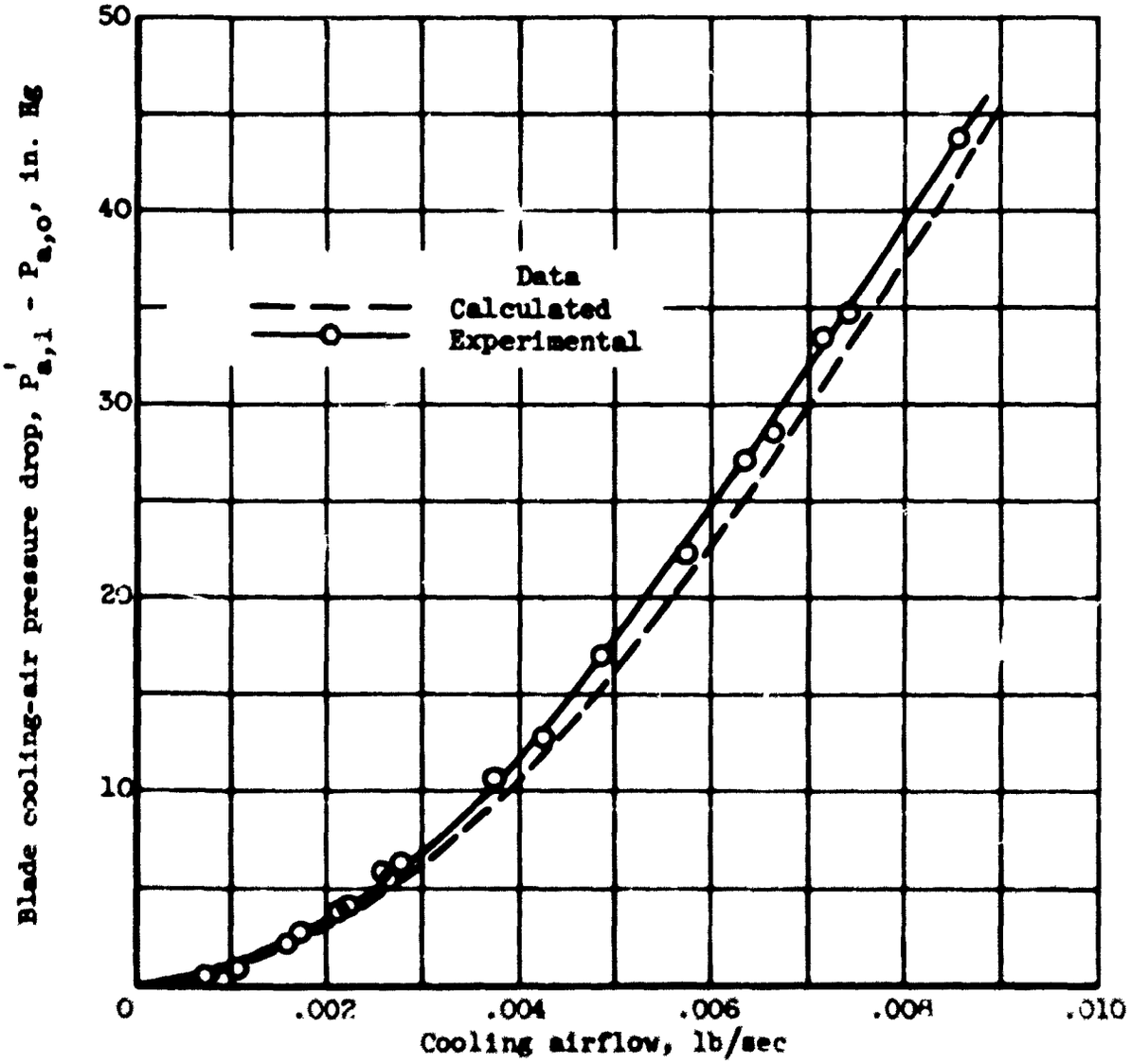

Figure 6. - Comparison of calculated blade cooling-air pressure drop with experimental data.

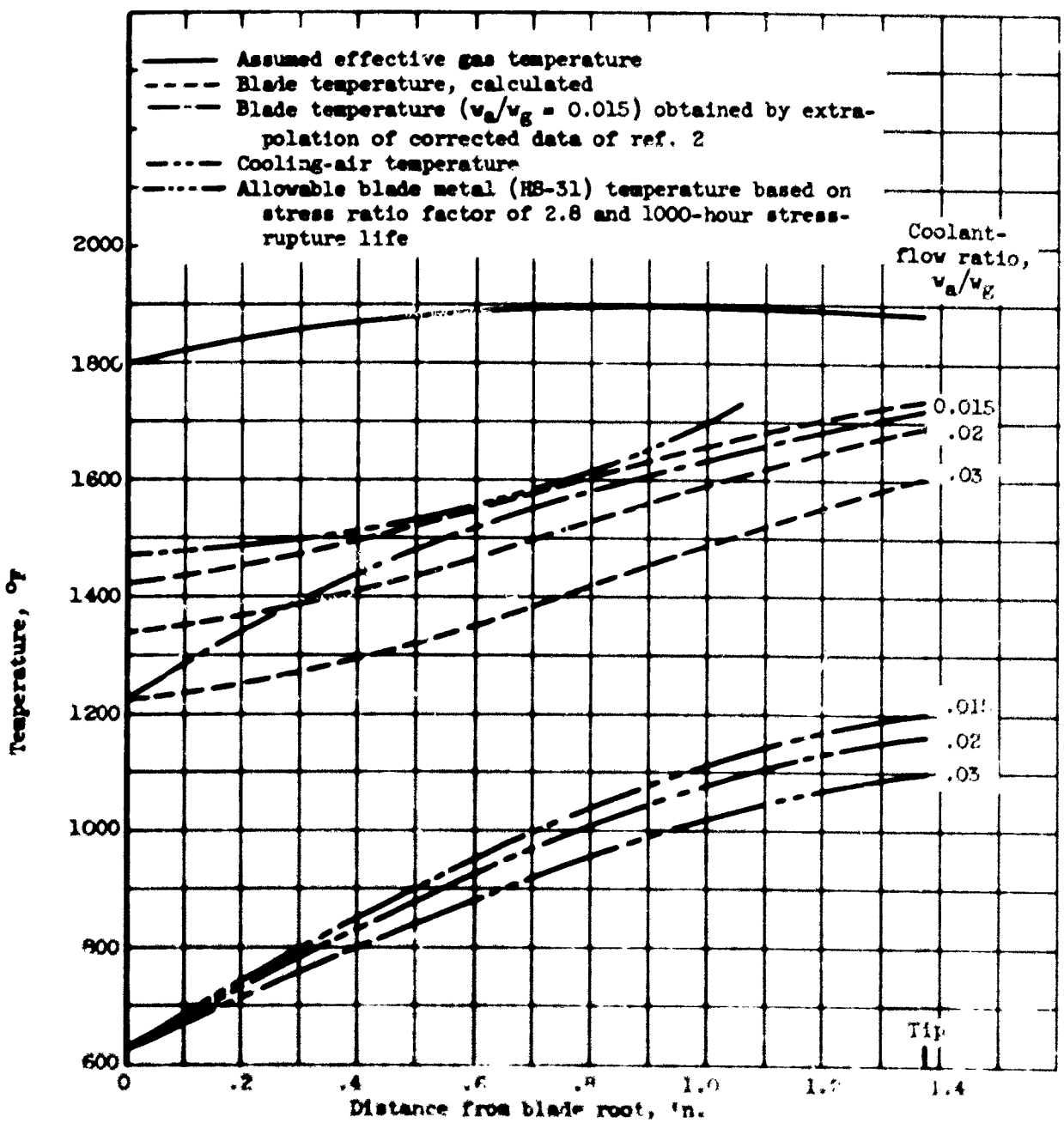

Figure 7. - Calculated blade metal and cooling-air spanwise temperature distributions over range of coolant-flow ratios for first-stage turbine rotor blade in a typical turboprop engine. Assumed flight conditions: 400 knots at 30,000-foot altitude.

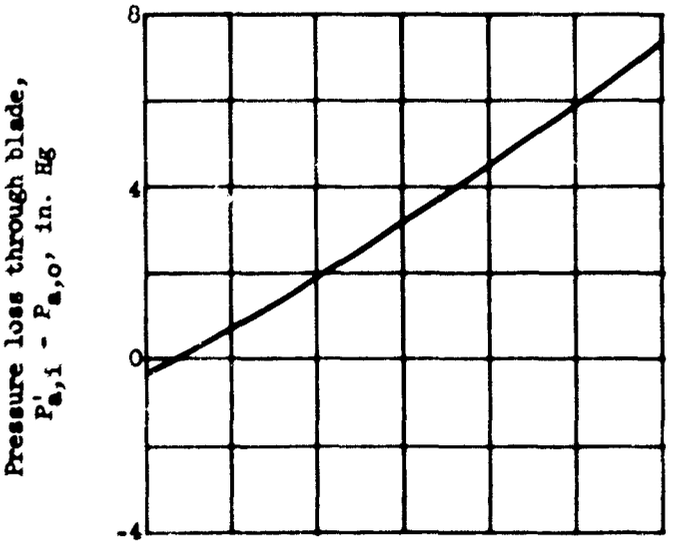

(a) Pressure loss through blade.

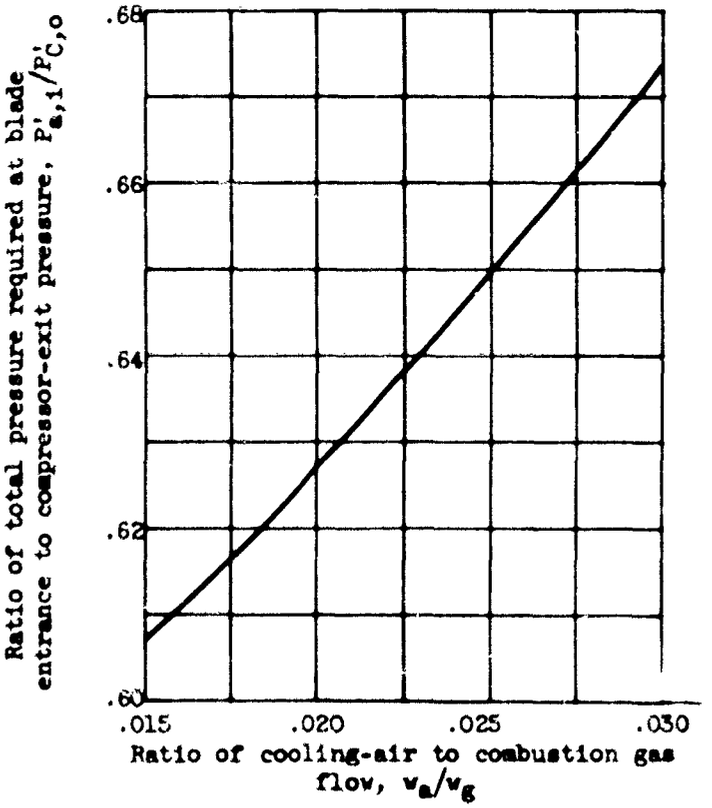

(b) Ratio of total pressure required at blade entrance to compressor-exit pressure.

Figure 8. - Calculated cooling-air pressure loss characteristics for cast finned turbine rotor blade for flight conditions of 300 knots at 30,000-foot altitude and turbine-inlet temperature of 2000° F for a typical turboprop engine.